

# Esculetin Alleviates IL-1 $\beta$ -Evoked Nucleus Pulposus Cell Death, Extracellular Matrix Remodeling, and Inflammation by Activating Nrf2/HO-1/NF- $\kappa$ b

Chunhui Huang,<sup>§</sup> Kaiwei Zou,<sup>§</sup> Yizhang Wang, Kai Tang, and Yiqi Wu\*



Cite This: *ACS Omega* 2024, 9, 817–827



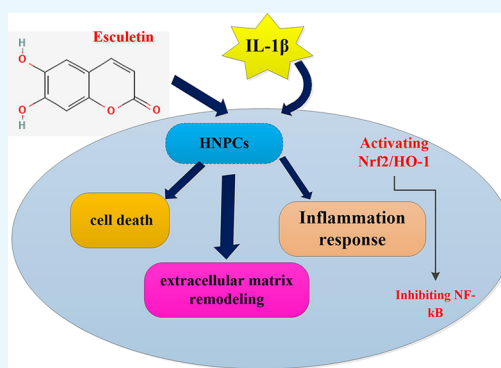
Read Online

ACCESS |

Metrics & More

Article Recommendations

**ABSTRACT:** Inflammation, extracellular matrix metabolic dysfunction, and oxidative stress are key pathogenic characteristics of intervertebral disk degeneration (IVDD), a major pathogenic cause of low back pain. Esculetin possesses anti-injury, anti-inflammation, and antinociceptive properties. This study aimed to explore its role in IVDD. In this research, esculetin exhibited little cytotoxicity to human nucleus pulposus cells (NPCs). Moreover, esculetin increased cell viability under IL-1 $\beta$  stimulation but attenuated IL-1 $\beta$ -induced cell apoptosis and caspase-3 activity. Furthermore, IL-1 $\beta$ -evoked increases in intracellular reactive oxygen species and malondialdehyde (MDA) levels, and decreases in superoxide dismutase (SOD) activity were reversed after esculetin treatment, indicating the antioxidative stress efficacy of esculetin. Esculetin alleviated the inhibitory effects of IL-1 $\beta$  on the transcription and protein expression of anabolic biomarkers (collagen II and aggrecan), accompanied by decreases in expression and release of catabolic biomarkers MMP-3 and MMP-13 from NPCs. Moreover, IL-1 $\beta$  exposure enhanced the expression levels of the inflammatory mediator nitric oxide and inflammatory cytokine IL-6 and TNF- $\alpha$ , which were overturned after esculetin treatment. Additionally, esculetin activated the nuclear factor-erythroid 2-related factor 2 (Nrf2)/heme oxygenase 1 (HO-1) to inhibit the activation of nuclear factor  $\kappa$ B (NF- $\kappa$ B) signaling in NPCs. Importantly, suppression of Nrf2 signaling reversed the protective efficacy of esculetin against IL-1 $\beta$ -mediated oxidative injury, matrix metabolism disruption, and inflammatory response in NPCs. Together, esculetin may alleviate IL-1 $\beta$ -induced dysfunction in NPCs by regulating the Nrf2/HO-1/NF- $\kappa$ B signaling, indicating its potential as a promising therapeutic agent against IVDD.



## INTRODUCTION

The intervertebral disk (IVD) is an essential soft connective tissue in the spine and can transmit loads caused by body weight and muscle activity via the spinal column. The degeneration of IVD, also known as intervertebral disk degeneration (IVDD), is the most prevalent disease among middle-aged and elderly people and serves as a major cause and basic inducement of a range of low back/neck pain.<sup>1</sup> Epidemiological studies reveal that approximately 12% of adults experience low back pain (LBP) in their lifetime worldwide, and this prevalence is even higher in people over 60 years of age, ranging from 21 to 75%.<sup>1,2</sup> Notably, the direct and indirect economic burden for low back pain caused by IVDD exceeds \$100–200 billion annually in the United States and 82.14 billion yen in Japan.<sup>3,4</sup> It is estimated that the incidence of LBP is likely to increase substantially due to the aging of the population in the coming decades.<sup>1</sup> Currently, low back pain caused by IVDD constitutes a major global healthcare concern causing higher disability than other medical conditions.<sup>5</sup>

Central nucleus pulposus (NP) is a major participant in IVD and is composed of NP cells and extracellular matrix (ECM)

components. As a critical contributor, NP cells are typically situated in a gelatinous matrix within NP and can secrete abundant proteoglycans (e.g., aggrecan) and type II collagen to maintain the body's resistance to axial compression and spinal pressure. The degeneration of NP is a critical pathogenic factor for the progression of IVDD that is closely related to oxidative stress and subsequent apoptosis of NP cells.<sup>6,7</sup> Furthermore, the degeneration process of IVDD is usually accompanied by an inflammatory response, which is central to pain and degeneration in IVDD.<sup>5,7</sup> The increased inflammatory mediators are present in human IVDD, such as interleukin-1 $\beta$  (IL-1 $\beta$ ).<sup>5,8</sup> Exposure of NP cells to an inflammatory environment will induce dysfunction and subsequent production of abundant proinflammatory cytokines, leading to the

**Received:** September 7, 2023

**Revised:** November 21, 2023

**Accepted:** November 29, 2023

**Published:** December 18, 2023



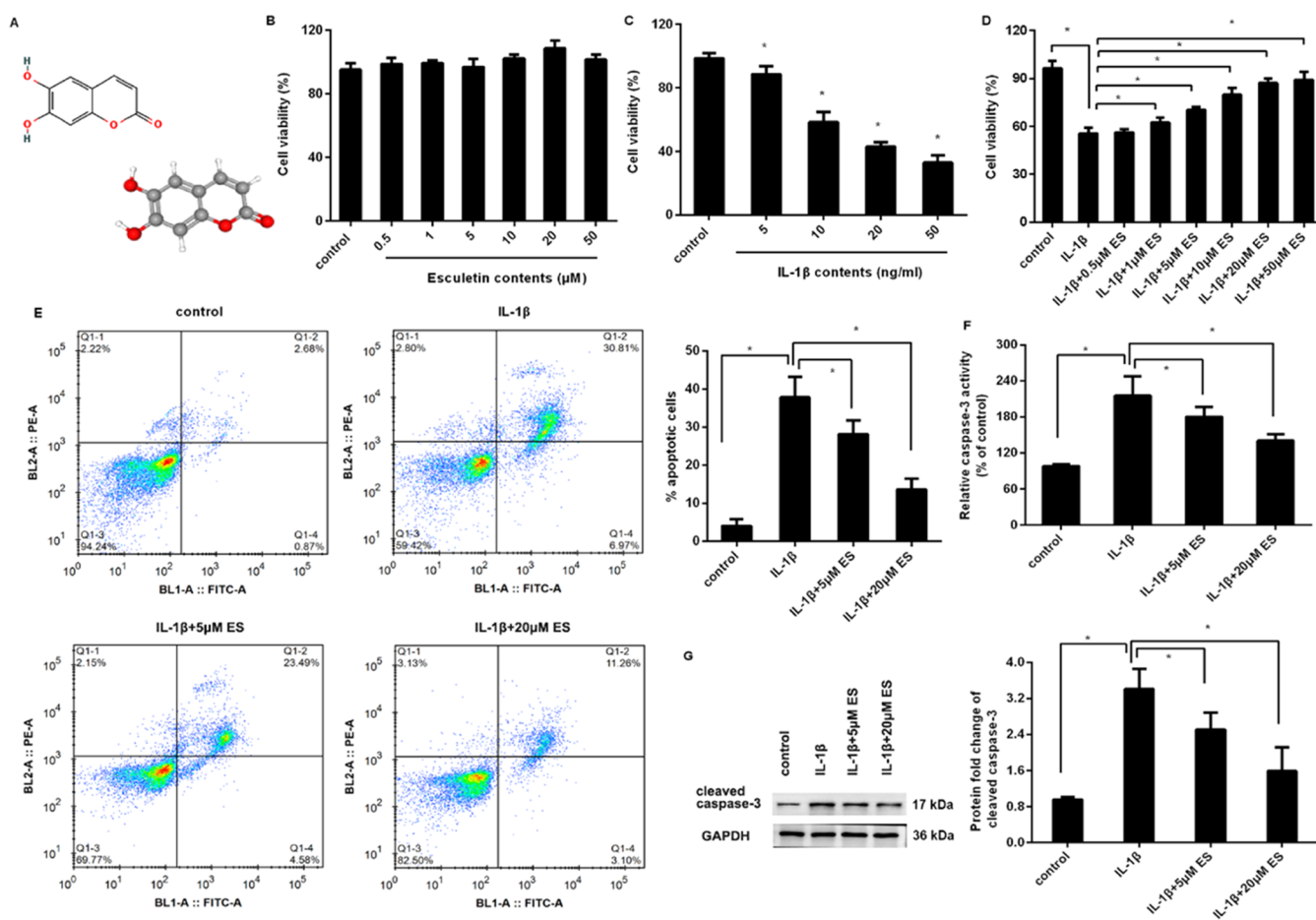


**Figure 1.** Esuletin protected against IL-1 $\beta$ -evoked apoptosis but had little cytotoxicity to HNPCs. (A) 2D and 3D chemical structures of esuletin. (B) Cytotoxicity of esuletin on HNPCs was analyzed. (C) Cells were exposed to various doses of IL-1 $\beta$ . Cell viability was then determined. (D) Cells were treated with 10 ng/mL of IL-1 $\beta$  and esuletin ranging from 0.5 to 50  $\mu$ M for 24 h. Then, a CCK-8 assay was performed to detect cell viability. (E, F) Cell apoptosis (E) and caspase-3 activity were evaluated. (G) Protein expression of cleaved caspase-3 was analyzed by Western blotting assay. \* $P < 0.05$ .

enhanced inflammatory response during the progression of IVDD.<sup>7,9</sup> Importantly, inflammatory exposure or other pathogenic stimuli will cause an imbalance in matrix synthesis and degradation within NP cells by increasing the catabolic enzyme matrix metalloproteinases (MMPs) and decreasing the synthesis of collagen, ultimately leading to the degradation of IVD.<sup>6,10</sup> Therefore, elucidating the mechanism underlying NP cell dysfunction is a promising strategy for the treatment of IVDD.<sup>6,10</sup>

As a natural dihydroxy coumarin (Figure 1A), esuletin is one of the main effective ingredients of common Chinese herbal medicines, such as *Artemisia capillaris*, *Cortex fraxini*, and *Fraxinus rhynchophylla* Hance, which are widely used in Asian countries.<sup>11</sup> Abundant evidence highlights that esuletin exerts a wide range of pharmacological properties in multiple progression of diseases, such as cardiovascular disease, cancer and diabetes.<sup>11</sup> Intriguingly, esuletin has been implicated in a diversity of biological effects, including antioxidation and anti-inflammation.<sup>12</sup> For instance, esuletin protects against hypoxia/reoxygenation-induced oxidative injury and apoptosis of cardiomyocytes.<sup>12</sup> Moreover, administration with esuletin alleviates doxorubicin-induced cardiotoxicity,<sup>13</sup> neurotoxicity,<sup>14</sup> and lipopolysaccharide (LPS)-induced lung injury.<sup>15</sup> Moreover, esuletin plays the anti-inflammatory roles in colitis<sup>16</sup> and sepsis.<sup>17</sup> Intriguingly, treatment with esuletin

exerts antinociceptive properties in inflammatory pain models of rats.<sup>18</sup> Moreover, esuletin can mitigate inflammatory response in macrophages by activating the nuclear factor (erythroid 2)-related factor 2 (Nrf2).<sup>19</sup> Additionally, esuletin alleviates cartilage destruction in experimental osteoarthritis by inhibiting the production of MMPs.<sup>20</sup> However, its role in IVDD remains unclear. In this study, we sought to investigate the effects of esuletin on cell injury, disorder in extracellular matrix metabolism, and inflammatory response in IVDD *in vitro* by exposing human nucleus pulposus cells (HNPCs) to IL-1 $\beta$ .

## MATERIALS AND METHODS

**Cell Culture and Stimulation.** The HNPCs were obtained from ScienCell Research Laboratories (no. 4800; ScienCell, TX) and used within the first three passages for the following experiments. All cells were maintained in Dulbecco's modified Eagle's medium (DMEM) supplemented with 10% fetal bovine serum (Gibco, Waltham, MA) and antibiotics (1% penicillin/streptomycin) in a 5% CO<sub>2</sub> incubator at 37 °C. For the stimulation, cells were exposed to multiple doses of esuletin (0.5–50  $\mu$ M) ( $\geq 95\%$  purity; National Institutes for Food and Drug Control; Beijing, China) and/or IL-1 $\beta$  (Sigma Chemical Co., MO) for 24 h.

**siRNA Transfection.** To induce the knockdown of Nrf2 in HNPCs, siRNA transfection was performed. Briefly, HNPCs at 70–80% confluency were inoculated into a six-well plate. Then, cells were transfected with siRNAs targeting Nrf2 or scramble control (No. 107966; Invitrogen, Carlsbad, CA) using Lipofectamine RNAi MAX (5  $\mu$ L; Invitrogen). The scrambled siRNAs were applied as the negative control (si-NC). After the above incubation for 48 h, all specimens were harvested to evaluate the final transfection efficacy of siRNAs using the Western blotting assay.

**Cell Counting Kit (CCK)-8 Detection.** Cytotoxicity on HNPCs was assessed by the CCK-8 kits (#G021-1-1; Nanjing Jiancheng Bioengineering Institute, Nanjing, China). All protocols were performed according to the manufacturer's instructions. Briefly, the cells were transfected with si-Nrf2 under esculetin or 10 ng/mL IL-1 $\beta$  exposure for 24 h. Then, a culture medium containing 10  $\mu$ L of the CCK-8 solution was added for further reaction. Four hours later, the wavelength of 450 nm was captured using a microplate reader.

**Cell Apoptosis Analysis.** Cell apoptosis was detected according to the previously described method.<sup>21,22</sup> HNPCs within a six-well plate were transfected with si-Nrf2 under IL-1 $\beta$  and esculetin exposure for 24 h. Then, the cells were harvested and centrifuged for 5 min. Subsequently, the cells were resuspended in a 1 $\times$  Annexin V binding buffer (100  $\mu$ L) and then incubated with 5  $\mu$ L of Annexin V-FITC and 10  $\mu$ L of PI (#C1062S; Beyotime, Shanghai, China) avoiding light. Fifteen minutes later, all samples were subjected to an LSRII flow cytometer (BD Biosciences) and analyzed with CellQuest software. All experimental procedures were carried out according to the protocols of Annexin V Apoptosis Kits (Beyotime).

**Detection of the Caspase-3 Activity.** The activity of caspase-3 in HNPCs was determined using a commercial Caspase-3 Activity Detection Kit (#G015-1-3; Nanjing Jiancheng Bioengineering Institute). All experimental protocols were performed according to the manufacturer's instructions. After the collection of HNPCs under various treatments, the cells were lysed with ice-cold lysis buffer. Then, the prepared lysates were incubated with 10  $\mu$ L of Ac-DEVD-pNA, a specific substrate of caspase-3, at 37  $^{\circ}$ C. Four hours later, the activity of caspase-3 was evaluated by detecting the absorbance at 405 nm.

**qRT-PCR.** A TRIzol reagent (Beyotime) was applied to extract total RNA from HNPCs that was then used as a template to prepare the first-strand complementary DNA (cDNA) using SuperScript II First-Strand Synthesis System (Invitrogen). Then, the mRNA levels of collagen II, aggrecan, MMP-3, MMP-13, inducible nitric oxide synthase (iNOS), IL-6, and tumor necrosis factor- $\alpha$  (TNF- $\alpha$ ) were quantified using SYBR Premix Ex Taq Kit (Sangon, Shanghai, China) according to the manufacturer's protocols. The primers involved in experiments were shown as follows: collagen II (sense, 5'-CAGCAAGAGCAAGGAGAAGA-3'; antisense, 5'-CAGTGTGTTGGGAGCCAGATT-3'), aggrecan (sense, 5'-CACAAGGGAGAGAGGGTAGT-3'; antisense, 5'-GGACGAAAGGGAGATGGAAAG-3'), IL-6 (sense, 5'-GGAGACTTGCCCTGGTGAAA-3'; antisense, 5'-CTGGCTTGTTCCTCACTACTC-3'), TNF- $\alpha$  (sense, 5'-CTCAACGGACTCAGCTTTCT-3'; antisense, 5'-GTCTGTGGTCTGTTTCTCT-3'), iNOS (sense, 5'-TGGAGCGAGTTGTGGATTG-3'; antisense, 5'-CCTCTTGTCTTTGACCCAGTAG-3'), MMP-3 (sense, 5'-

GTGAGGACACCAGCATGAA-3'; antisense, 5'-GACCACTGTCCTTTCTCCTAAC-3'), MMP-13 (sense, 5'-GGAAGAAGAGCTATCAGGAGAAAG-3'; antisense, 5'-CCAGCCACGCATAGTCATATAG-3'), and glyceraldehyde-3-phosphate dehydrogenase (GAPDH) (sense, 5'-GTCAACGGATTTGGTTCGTATTG-3'; antisense, 5'-CCGTTCTCAGCCATGTAGTT-3'). The formula  $2^{-\Delta\Delta Ct}$  was used to quantify the transcripts of targeted genes with a normalization control of GAPDH.

**Detection of Intracellular Reactive Oxygen Species (ROS), Malondialdehyde (MDA), and Superoxide Dismutase (SOD) Content Levels.** The levels of ROS in cells were determined according to the previously described method.<sup>23,24</sup> Briefly, to detect ROS levels, a serum-free culture medium containing 10  $\mu$ M DCFH-DA (#S0033S; Beyotime) was added to yield fluorescent DCF. Approximately 30 min later, a fluorescence microscope (Nikon, Tokyo, Japan) and a fluorometric microplate reader (Molecular Devices, Sunnyvale, CA) were used to measure fluorescence with the excitation wavelength of 490 nm and emission wavelength of 525 nm.

For the measurements of MDA (#A003-4-1) and SOD activity (#A001-1-1), the commercial kits were obtained from Nanjing Jiancheng Bioengineering Institute. To determine the levels of MDA, all specimens were treated with reacted reagents and then incubated at 95  $^{\circ}$ C for 40 min. After centrifugation for 10 min, the supernatants were collected, and the absorbance at 532 nm was analyzed. For the analysis of SOD, all samples were incubated at 37  $^{\circ}$ C for 20 min. Then, the absorbance at 450 nm was captured to determine the SOD activity.

**Measurement of Nitric Oxide (NO) Levels.** Following the various treatments, HNPCs were collected and incubated with a Griess reaction (#A012-1-2; Nanjing Jiancheng Bioengineering Institute) for 10 min. Then, the contents of nitrite were spectrophotometrically measured to determine the NO levels by capturing the absorbance at 550 nm. The detailed procedures were performed according to the instructions of the commercial NO detection kits.

**Western Blotting Assay.** Protein expression was analyzed according to the previously described method.<sup>25,26</sup> Briefly, a solution of RIPA lysis buffer was added to extract the total protein from HNPCs. A commercial BCA protein kit (Beyotime) was used to quantify the prepared protein concentration. Next, approximately 35  $\mu$ g of protein samples were subjected to 12% sodium dodecyl sulfate-polyacrylamide gel electrophoresis (SDS-PAGE) gel and transferred to a PVDF membrane (Bio-Rad; Hercules, CA). Then, the membranes were interdicted with 5% nonfat milk for 1.5 h before the incubation with the primary antibodies against human collagen II (1:8000; #ab188570), aggrecan (1:3000; #ab3778), MMP-3 (1:10000; #ab52915), MMP-13 (1:5000; #ab39012), Nrf2 (1:1000; #ab137550), heme oxygenase 1 (HO-1) (1:2000; #ab52947), Lamin B (1:1000; #ab229025), cleaved caspase-3 (1:500; #ab32042) (all from Abcam, Cambridge, U.K.), p65 nuclear factor kappa-B (NF- $\kappa$ B) (1:1000; #sc-8008), and phosphorylated p65 NF- $\kappa$ B (p-p65) (1:1500; #sc-166748) (from Santa Cruz Biotechnology; Santa Cruz, CA). After incubation at 4  $^{\circ}$ C overnight, the membranes were rinsed and incubated with horseradish peroxidase (HRP)-conjugated second antibody at room temperature for 2 h. The binding sites were then visualized using the enhanced chemiluminescence ECL reagent (No. P0018S; Beyotime) and analyzed using a Gel Doc XR imaging system (Bio-Rad

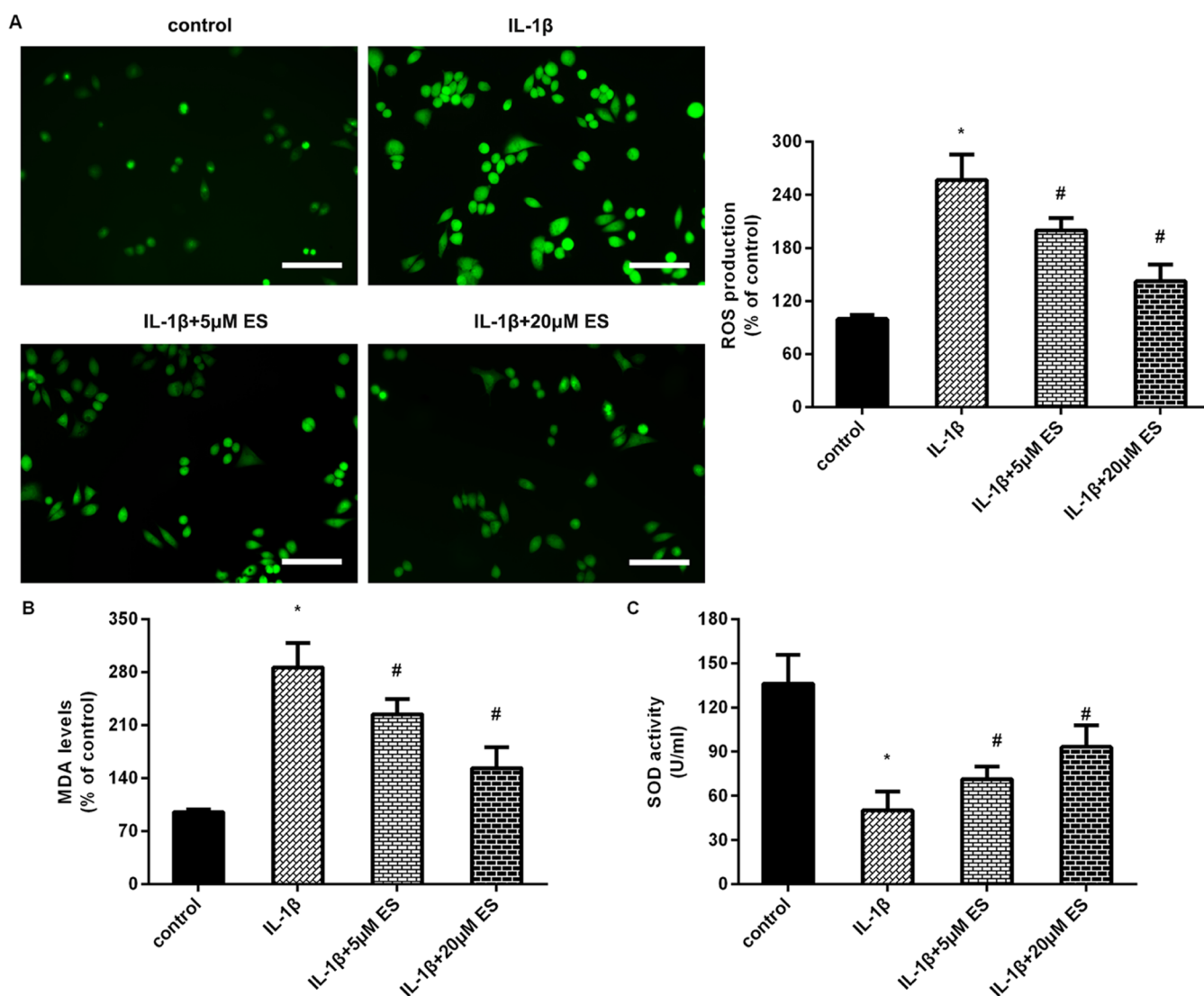


**Figure 2.** Esuletin treatment ameliorated the IL-1 $\beta$ -induced oxidative stress in HNPCs. Cells were treated with 10 ng/mL of IL-1 $\beta$  and esuletin (5 and 20  $\mu$ M) for 24 h. Then, the levels of ROS (A) were determined by detecting the generated fluorescent DCF. Furthermore, the contents of MDA (B) and SOD activity (C) were assessed in HNPCs using the corresponding commercial kits. Scale bar = 50  $\mu$ m. \* $P$  < 0.05 vs control groups. # $P$  < 0.05 vs IL-1 $\beta$  groups.

Laboratories, Hercules, CA) and ImageJ software. The endogenous control of GAPDH was introduced to normalize the targeted proteins.

**ELISA Analysis.** The contents of inflammatory cytokines (TNF- $\alpha$  and IL-6) in supernatants from HNPCs were quantified using the TNF- $\alpha$  (#DTA00D) and IL-6 (#D6050) ELISA Kits (R&D Systems, Minneapolis, MN). Human ELISA kits for MMPs (MMP-3 and MMP-13) were obtained from ebioscience (#BMS2014-3 and #EHMMP13; San Diego, CA). Detailed experimental procedures were performed according to the manufacturer's recommendations. Briefly, the supernatants from cells were prepared by centrifuging for 10 min to remove cell fragments. Then, 50  $\mu$ L of the prepared samples were added into 96-well plates and then incubated with human TNF- $\alpha$ , IL-6, MMP-3, and MMP-13 HRP and biotin conjugates (100  $\mu$ L) at 37  $^{\circ}$ C for 1 h. Subsequently, the substrate solution was added for further incubation for 15–20 min under dark. Then, the stopping solution (50  $\mu$ L) was added and the absorbance at 450 nm was spectrophotometrically measured with a microplate reader.

**Statistical Analysis.** All data from at least three individual experiments are presented as the mean  $\pm$  standard deviation (SD). The statistical analysis was carried out using SPSS version 20.0 software. Data were statistically analyzed using ANOVA with posthoc SNK test for comparison in multiple groups.  $P$  < 0.05 was defined as a statistical significance.

## RESULTS

### Esuletin Antagonizes IL-1 $\beta$ -Evoked HNPC Cell Apoptosis while Having Little Cytotoxicity to Cells.

The chemical structure of esuletin is shown in Figure 1A. To further elaborate on the function of esuletin in the development of IVDD, we first investigated its roles in IVDD *in vitro* by constructing an IL-1 $\beta$ -evoked HNPC model. Before this, we first explored the cytotoxicity of esuletin in HNPCs and confirmed that exposure to esuletin ranging from 0.5 to 50  $\mu$ M resulted in little cytotoxicity to HNPCs (Figure 1B). Cells stimulated with IL-1 $\beta$  exhibited a remarkable decrease to 58.62% in cell viability when the dose was up to 10 ng/mL, while cell viability was further inhibited when the dose

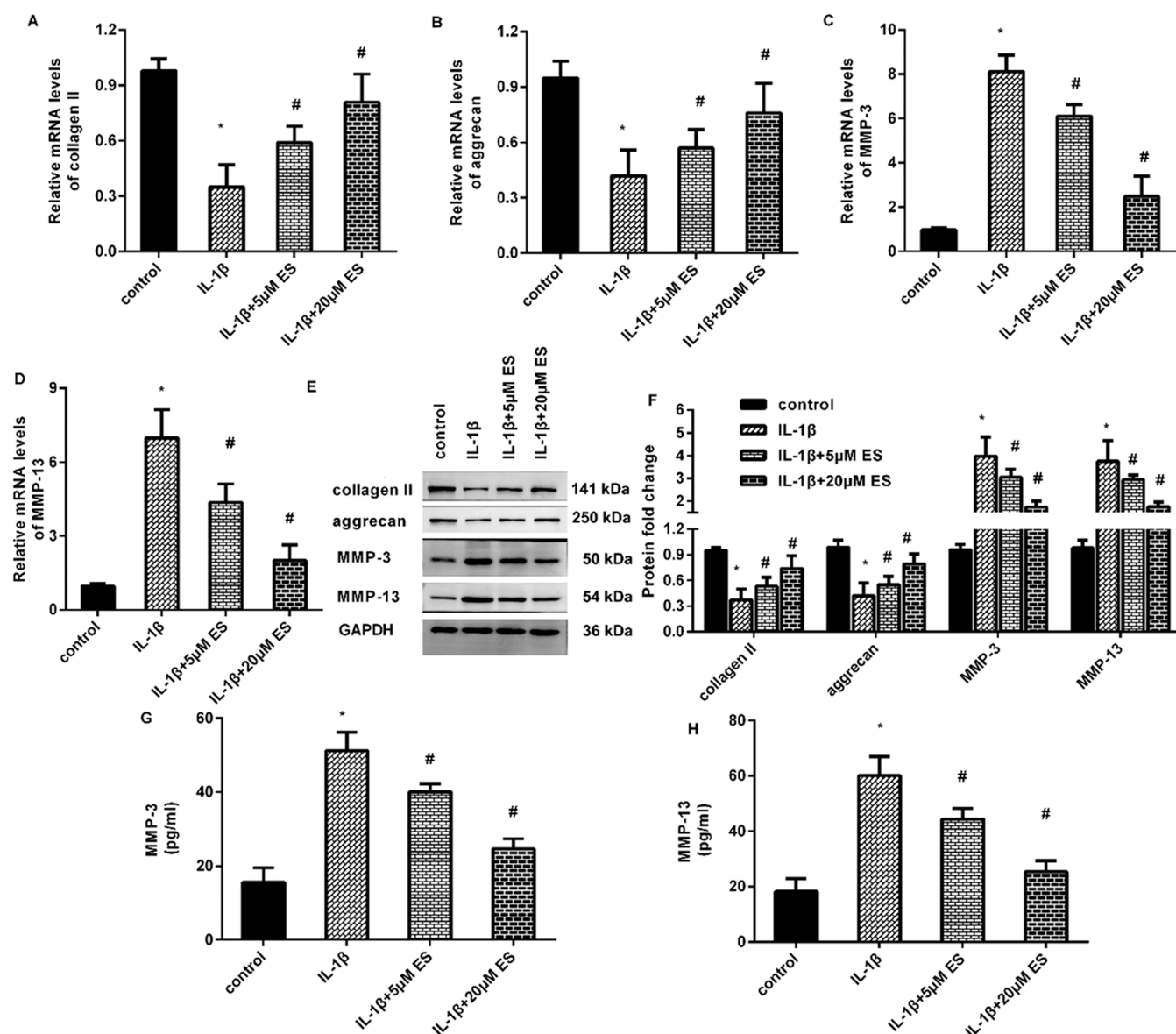


**Figure 3.** Escluletin regulated the extracellular matrix metabolism disorder in IL-1 $\beta$ -stimulated HNPCs. (A–D) HNPCs were treated with 10 ng/mL IL-1 $\beta$  and various doses of escluletin. Approximately 24 h later, the mRNA levels of anabolic biomarkers (collagen II and aggrecan) (A, B) and catabolic biomarkers (MMP-3 and MMP-13) (C, D) were detected by qRT-PCR. (E, F) Western blotting assay was performed to determine the protein levels. (G, H) Releases of MMP-3 (G) and MMP-13 (H) from HNPCs were analyzed. \* $P$  < 0.05 vs control groups. # $P$  < 0.05 vs IL-1 $\beta$  groups.

of IL-1 $\beta$  was greater than 10 ng/mL (Figure 1C). Therefore, the concentration of 10 ng/mL was selected for the following experiments. In contrast to the control groups, IL-1 $\beta$  exposure inhibited cell viability; however, escluletin over 1  $\mu$ M significantly reversed the IL-1 $\beta$ -evoked inhibition of cell viability (Figure 1D). No obvious differences were observed in 20  $\mu$ M- and 50  $\mu$ M-treated groups. Additionally, IL-1 $\beta$  stimulation increased cell apoptosis relative to the control groups, which was reversed after escluletin treatment at doses of 5 and 20  $\mu$ M (Figure 1E). The increased activity of caspase-3 in IL-1 $\beta$ -exposed HNPCs was also dose-dependently attenuated after escluletin treatment (Figure 1F). Furthermore, exposure to IL-1 $\beta$  enhanced the protein expression of cleaved caspase-3 in HNPCs, which was reversed by escluletin (Figure 1G).

**Escluletin Alleviates IL-1 $\beta$ -Induced Oxidative Stress in HNPCs.** Further analysis confirmed that IL-1 $\beta$  exposure induced 2.56-fold increases in ROS levels relative to the control groups; however, this increase was overturned after treatment with 5 and 20  $\mu$ M escluletin (Figure 2A). Moreover, the increased contents of MDA, a marker of oxidative stress, were observed in IL-1 $\beta$ -stimulated cells, which were dose-dependently inhibited after escluletin administration (Figure 2B). Importantly, the activity of the antioxidative enzyme SOD was reduced after IL-1 $\beta$  treatment (Figure 2C). Nevertheless, the suppressive effects of IL-1 $\beta$  on SOD activity were muted following escluletin treatment (Figure 2C). Thus, these data support the antioxidative stress efficacy of escluletin in HNPCs under inflammatory conditions.

**Escluletin Regulates Extracellular Matrix Metabolic Dysfunction in HNPCs in Response to IL-1 $\beta$  Exposure.**

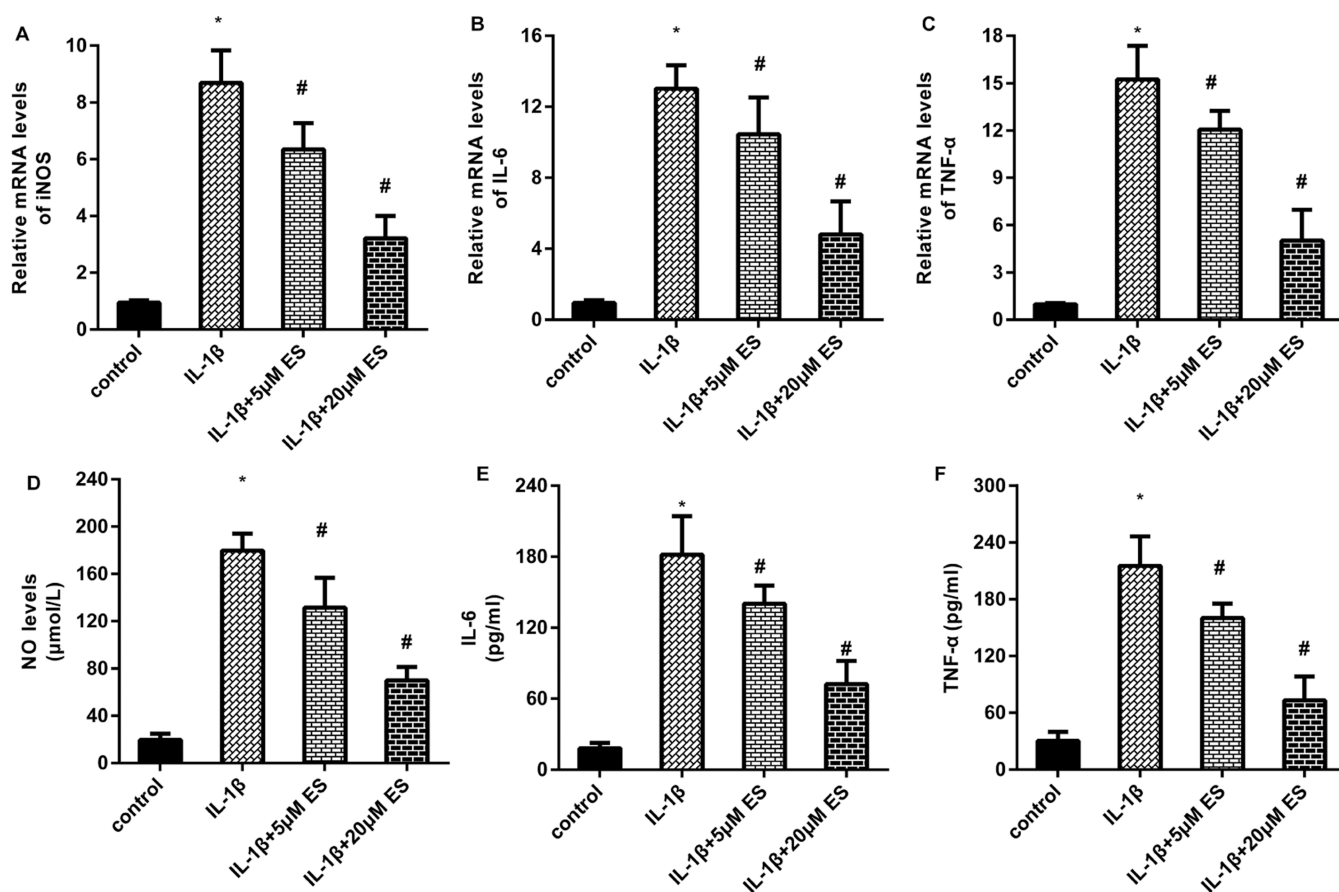


**Figure 4.** Esculetin inhibited the inflammatory response in IL-1 $\beta$ -stimulated HNPCs. (A–C) mRNA levels of the inflammatory mediators were detected by qRT-PCR. (D–F) After the stimulation with IL-1 $\beta$  and esculentin for 24 h, the production of NO (D), IL-6 (E), and TNF- $\alpha$  (F) from HNPCs was measured. \* $P < 0.05$  vs control groups. # $P < 0.05$  vs IL-1 $\beta$  groups.

Extracellular matrix destruction constitutes a major cause of the development of IVDD.<sup>27,28</sup> Therefore, we next elaborate on the effects of esculentin on extracellular matrix metabolic dysfunction in HNPCs. Compared with the control groups, cells exposed to IL-1 $\beta$  had lower transcripts of anabolic biomarkers (collagen II and aggrecan) (Figure 3A,B) but higher transcripts of catabolic biomarkers (MMP-3 and MMP-13) (Figure 3C,D). However, esculentin antagonized the IL-1 $\beta$ -evoked above changes in a dose-dependent manner. Concomitantly, the decreased protein expression of collagen and aggrecan and increased protein levels of MMP-3 and MMP-13 were offset after esculentin treatment in IL-1 $\beta$ -treated cells (Figure 3E,F). Moreover, IL-1 $\beta$ -induced releases of MMP-3 (Figure 2G) and MMP-13 (Figure 2H) from HNPCs were also inhibited after esculentin treatment.

**Administration with Esculetin Restrains the Inflammatory Response in IL-1 $\beta$ -Stimulated HNPCs.** As shown in Figure 4A, IL-1 $\beta$  exposure induced 8.69-fold increases in the level of iNOS mRNA in HNPCs relative to the control groups, which were dose-dependently decreased after esculentin treatment. Furthermore, IL-1 $\beta$  enhanced the transcripts of a proinflammatory cytokine, including IL-6 (Figure 4B) and TNF- $\alpha$  (Figure 4C). However, these increases were overturned after esculentin incubation. Concomitantly, the increased levels of NO (Figure 4D), IL-6 (Figure 4E), and TNF- $\alpha$  (Figure 4F) in IL-1 $\beta$ -treated cells were reversed when cells were treated with esculentin.

**Esculetin Treatment Enhanced the Activation of the Nrf2/HO-1 Pathway in NP Cells in Response to IL-1 $\beta$  Stimulation.** Accumulating evidence highlights the protective efficacy of Nrf2/HO-1 signaling in IVDD.<sup>29,30</sup> As shown in Figure 5A,B, IL-1 $\beta$  treatments exhibited little effect on the protein expression of Nrf2 in HNPCs. No obvious changes in the protein levels of HO-1 were observed in IL-1 $\beta$ -treated cells (Figure 5A,C). Noticeably, treatment with esculentin enhanced the protein expression of Nrf2 and HO-1, indicating the activation of Nrf2/HO-1 in HNPCs.

**Esculetin Suppresses the IL-1 $\beta$ -Induced Activation of the NF- $\kappa$ B Signaling via the Nrf2/HO-1 Axis.** Aberrant activation of the NF- $\kappa$ B signaling has been implicated in the development of IVDD.<sup>7</sup> In this study, IL-1 $\beta$  exposure induced the activation of NF- $\kappa$ B signaling by increasing the protein expression of p-p65 NF- $\kappa$ B (Figure 5A,D). Moreover, esculentin inhibited IL-1 $\beta$ -induced increases in the protein expression of p-p65 NF- $\kappa$ B. Importantly, targeting Nrf2 reversed the inhibitory effects of esculentin on the activation of the NF- $\kappa$ B pathway (Figure 5A,D), indicating that esculentin may restrain the IL-1 $\beta$ -induced activation of NF- $\kappa$ B signaling via the Nrf2/HO-1 axis.

**Blocking the Nrf2 Signaling Overturns the Protective Efficacy of Esculetin against IL-1 $\beta$ -Evoked Apoptosis, Metabolic Dysfunction, and Inflammation.** Further analysis revealed that esculentin antagonized IL-1 $\beta$ -mediated inhibition of cell viability, which was overturned after si-Nrf2 transfection (Figure 6A). Moreover, the suppressive efficacy of

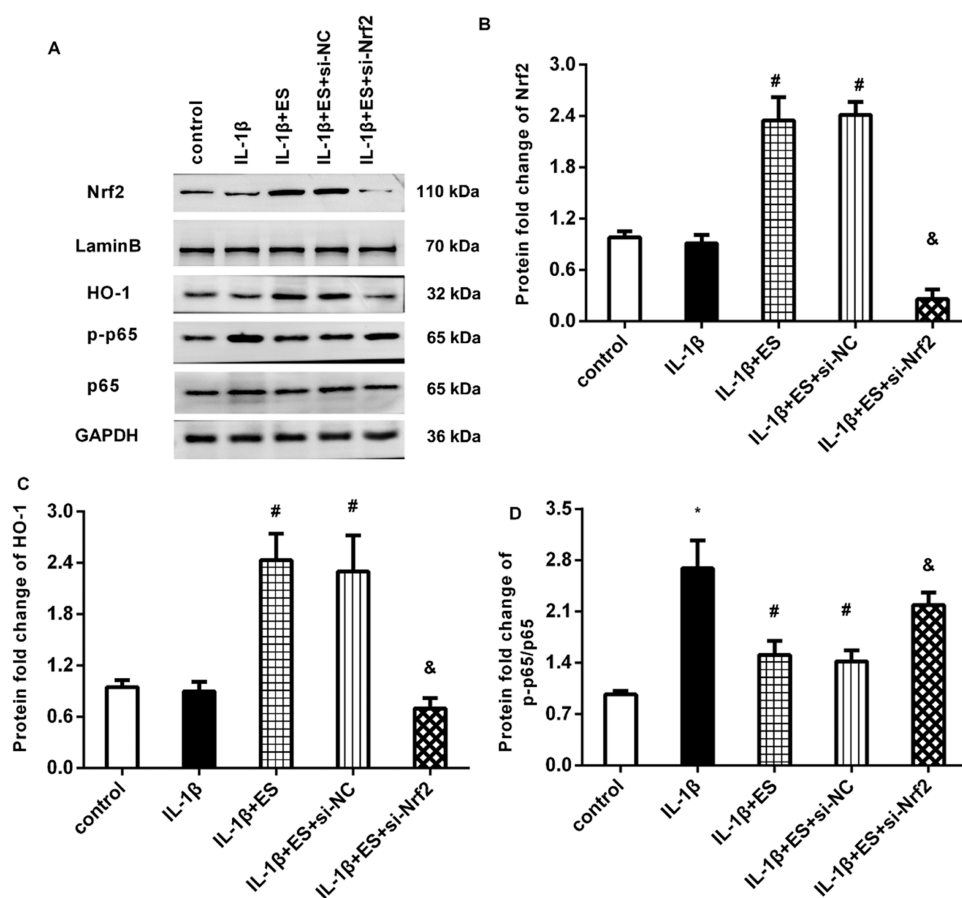


**Figure 5.** Esculetin suppressed the IL-1 $\beta$ -induced activation of NF- $\kappa$ B signaling via the Nrf2/HO-1 axis. HNPCs were transfected with si-Nrf2 for 48 h and exposed to IL-1 $\beta$  and esculentin conditions for 24 h. (A) Then, the protein expression levels of Nrf2, HO-1, p-p65 NF- $\kappa$ B, and p65 NF- $\kappa$ B were evaluated by Western blotting. (B–D) The corresponding bands were quantified using ImageJ software. \* $P < 0.05$  vs control groups. <sup>#</sup> $P < 0.05$  vs IL-1 $\beta$  groups. <sup>&</sup> $P < 0.05$  vs IL-1 $\beta$  and ES groups.

esculetin in IL-1 $\beta$ -induced apoptosis (Figure 6B) and ROS and MDA production (Figure 6C) were reversed after blocking the Nrf2 signaling. Concomitantly, the increased SOD activity in esculentin-stimulated cells under IL-1 $\beta$  conditions was reversed following the si-Nrf2 treatment (Figure 6D). Moreover, esculentin enhanced the protein expression of collagen II and aggrecan (Figure 7A) and mitigated MMP-3 and MMP-13 production (Figure 7B) in IL-1 $\beta$ -treated cells; however, these changes were offset after blocking the Nrf2 pathway. In addition, targeting Nrf2 signaling muted the inhibitory effects of esculentin on NO production (Figure 7C) and transcripts (Figure 7D) and the release (Figure 7E) of IL-6 and TNF- $\alpha$  in cells under IL-1 $\beta$  conditions.

## DISCUSSION

As a common degenerative disease, IVDD usually causes low back pain that affects the ability to work and quality of life worldwide.<sup>1</sup> IL-1 $\beta$  is a proverbial proinflammatory cytokine and is upregulated in NP tissues as the disk degeneration progresses, which may aggravate the development of IDD.<sup>5,8</sup> Therefore, IL-1 $\beta$  is usually used to mimic the progression of IVDD *in vitro*.<sup>6,10</sup> In this study, we investigated the roles of esculentin in IL-1 $\beta$ -induced dysfunction in NP cells and highlighted that esculentin protected HNPCs from IL-1 $\beta$ -induced oxidative injury, matrix metabolic disorder, and inflammation in HNPCs by blocking the NF- $\kappa$ B signaling via

the activation of the Nrf2/HO-1 axis. Thus, esculentin may be a promising agent for the treatment of IVDD.

NPCs are the dominant cell type in NP, and their death is a key contributor to IVDD. It has been demonstrated that the increase of ROS causes abundant oxidative stress, thus accelerating the degeneration of IVD.<sup>6,31</sup> Blocking oxidative stress in NPCs is becoming a promising strategy for the treatment of IVDD.<sup>6,32,33</sup> Consistent with previous findings,<sup>6,31,33</sup> IL-1 $\beta$  exposure enhanced the levels of ROS and MDA and decreased the activity of antioxidative SOD. Esculetin, a main effective ingredient from various Chinese herbal medicines, is involved in multiple biological processes, including antioxidative injury. For instance, esculentin ameliorates hypoxia-reoxygenation-induced apoptosis in cardiomyocytes by blocking oxidative stress.<sup>13</sup> In this study, esculentin had little cytotoxicity to HNPCs. Importantly, esculentin attenuated IL-1 $\beta$ -induced oxidative injury and cell apoptosis in HNPCs, indicating the antioxidative injury effects of esculentin on HNPCs. Intriguingly, esculentin retards LPS-induced lung injury.<sup>15</sup> Importantly, the antinociceptive efficacy of esculentin is demonstrated in a rat model of inflammatory pain.<sup>18</sup> These data indicate the beneficial potential of esculentin in IVDD by regulating oxidative injury in HNPCs.

The disruption of ECM metabolism in the IVD micro-environment usually leads to an imbalance in anabolic and catabolic processes, which is the major cause of IVDD.<sup>27,28</sup> Under normal conditions, ECM can maintain the internal

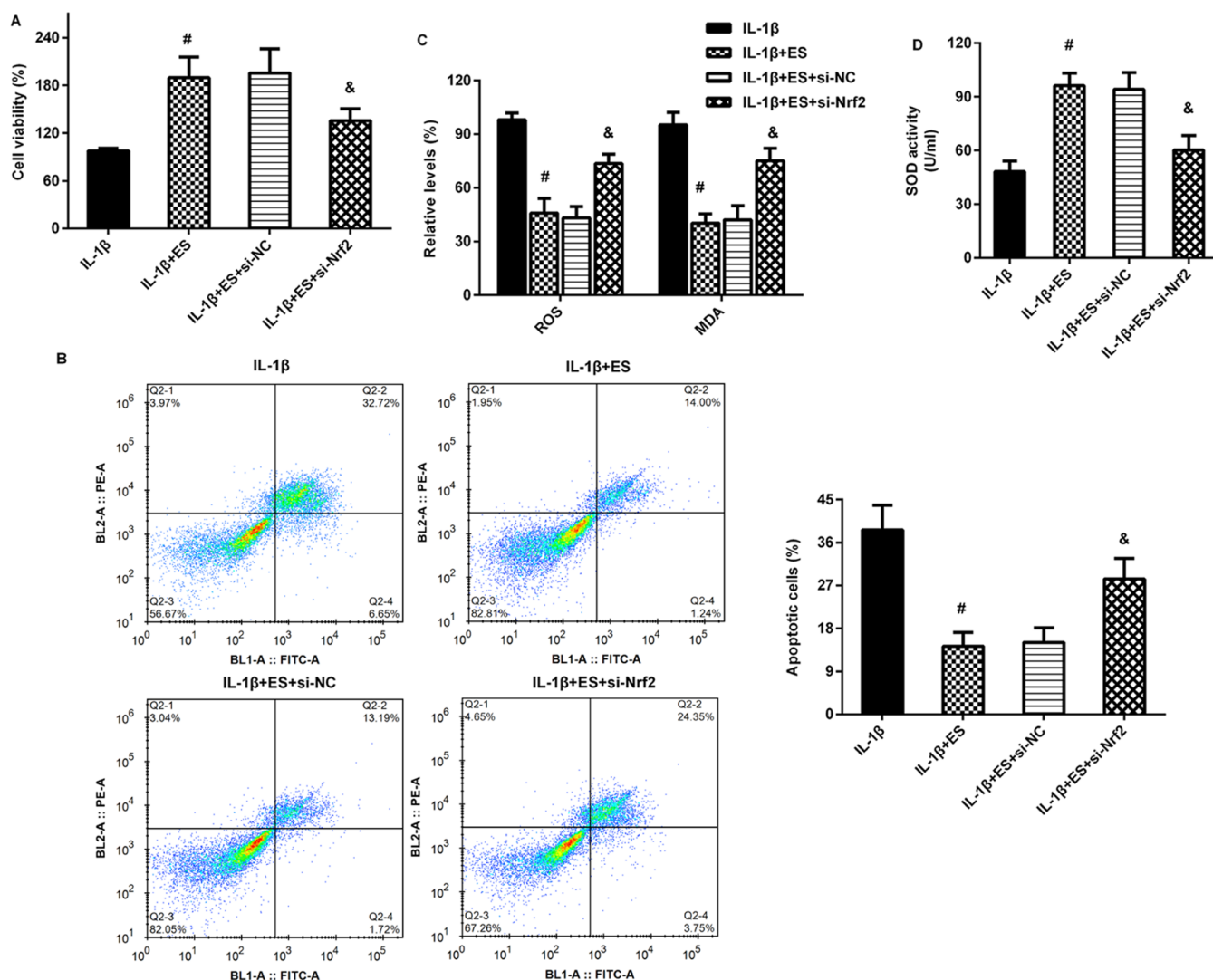


**Figure 6.** Blocking the Nrf2 signaling reversed the protective efficacy of esculentin against IL-1 $\beta$ -evoked apoptosis and oxidative injury. (A, B) Cells under IL-1 $\beta$  and esculentin conditions were transfected with si-Nrf2. Approximately 24 h later, cell viability (A) and apoptosis (B) were determined. The effects on oxidative stress were evaluated by detecting the levels of ROS, MDA (C), and SOD (D). <sup>#</sup> $P < 0.05$  vs IL-1 $\beta$  groups. <sup>&</sup> $P < 0.05$  vs IL-1 $\beta$  and ES groups.

pressure of the IVD by forming a powerful hydrodynamic system to fulfill the function of disks. During the development of IVDD, abundant productions of pro-catabolic enzyme MMPs and decreases of collagen II and proteoglycan (e.g., aggrecan) from NPCs will result in the metabolic function tilting toward catabolism from anabolism, leading to the disruption of ECM balance. Currently, increasing research has achieved their therapeutic efficacy for IVDD by affecting metabolic remodeling in ECM.<sup>10,27</sup> Similar to previous findings,<sup>6,10</sup> IL-1 $\beta$  stimulation increased the expression and release of catabolic biomarkers (MMP-3 and MMP-13) and decreased the expression of anabolic metabolism-associated collagen II and aggrecan, indicating the metabolic disruption toward catabolism in HNPCs. Notably, treatment with esculentin ameliorated IL-1 $\beta$ -evoked metabolic dysfunction by inhibiting IL-1 $\beta$ -induced catabolism-related expression of MMP-3 and MMP-13 and reversed IL-1 $\beta$ -mediated reduction of anabolic metabolism-associated collagen II and aggrecan expression. Thus, these data indicate that esculentin may regulate metabolic dysfunction in IL-1 $\beta$ -treated NPCs by suppressing excessive catabolism and increasing anabolism.

Intriguingly, a previous study confirmed that esculentin inhibited proteoglycan metabolism by blocking the production of MMPs in chondrocytes.<sup>34</sup> Additionally, administration with esculentin inhibits the expression of MMPs and therefore alleviates cartilage destruction in experimental osteoarthritis.<sup>20</sup>

As a key participator, inflammatory response usually occurs after injury and influences various pathogenic processes, such as cancer, IVDD, and IVDD-evoked pain, by inducing abundant releases of proinflammatory mediators and cytokines.<sup>5,9,35</sup> A growing body of evidence supports the fact that IVDD is commonly accompanied by increased levels of proinflammatory cytokines, such as IL-1 $\beta$ .<sup>7,36</sup> Notably, abundant production of these inflammatory factors will induce a local inflammatory response, which facilitates the catabolism of ECM and leads to the dysfunction and structural changes of IVD.<sup>31,37</sup> For instance, inflammatory mediator iNOS plays an important role in the inflammatory processes via accelerating the production of NO, thereby triggering the progression of IVDD.<sup>38</sup> In this study, IL-1 $\beta$  exposure enhanced the expression levels of inflammatory mediator iNOS, NO, and inflammatory cytokine IL-6 and TNF- $\alpha$  in human NPCs. Similar to these



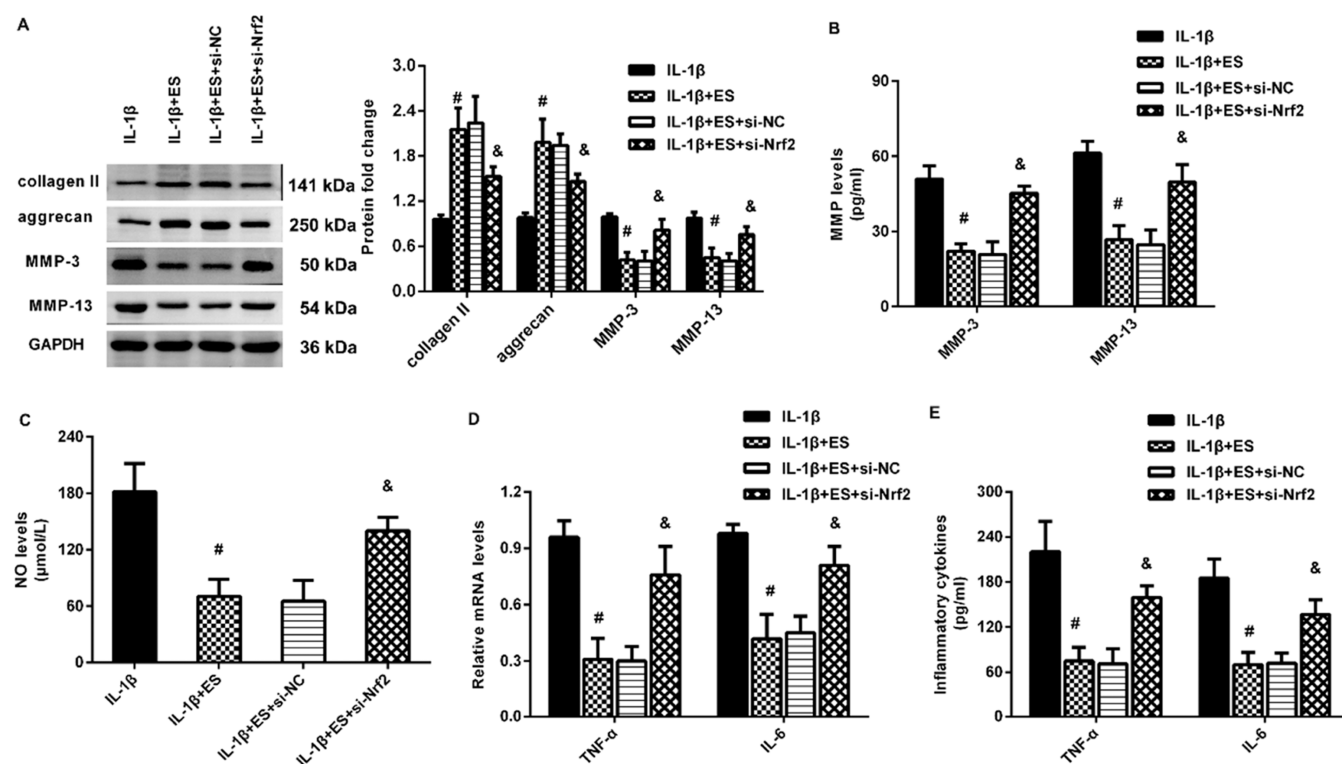


**Figure 7.** Targeting the Nrf2 pathway overturned the protective efficacy of esculentin against IL-1 $\beta$ -induced metabolic dysfunction and inflammation. (A) HNPCs were transfected with si-Nrf2 and incubated under IL-1 $\beta$  and esculentin conditions for 24 h. Then, the protein expression of extracellular matrix metabolic markers was analyzed by Western blotting. (B, C) Releases of MMPs (B) and NO (C) were determined. The transcript (D) and production (E) of inflammatory cytokines were measured. # $P$  < 0.05 vs IL-1 $\beta$  groups. & $P$  < 0.05 vs IL-1 $\beta$  and ES groups.

data, the previous study also revealed that IL-1 $\beta$  treatment increased the expression of these inflammatory mediators and cytokines in NPCs.<sup>29</sup> Esculetin has been proven to be involved in various pathogenic processes, including the anti-inflammatory response. For instance, esculentin can protect against early sepsis by inhibiting NF- $\kappa$ B-mediated inflammatory response.<sup>17</sup> Moreover, esculentin also alleviates LPS-induced inflammatory response and cell death in human retinal pigment epithelial cells.<sup>39</sup> In the present study, esculentin inhibited the inflammatory response in IL-1 $\beta$ -treated HNPCs. Increasing evidence supports anti-inflammation as a promising therapeutic approach against IVDD.<sup>5,10,36</sup> Thus, esculentin may attenuate the progression of IVDD by inhibiting the inflammatory response.

We next discerned the molecular mechanism underlying esculentin-mediated protection against IL-1 $\beta$ -induced dysfunction in HNPCs and confirmed that esculentin inhibited IL-1 $\beta$ -induced activation of NF- $\kappa$ B signaling. NF- $\kappa$ B is a common proinflammatory and multifunctional pathway and is recognized as a pathogenic factor for IVDD by regulating the NPC function.<sup>7</sup> Convincing evidence has substantiated that restraining the NF- $\kappa$ B signaling can alleviate the progression of IVDD.<sup>7,40</sup> Importantly, the current data confirmed that esculentin induced activation of the Nrf2/HO-1 axis in IL-1 $\beta$ -stimulated NPCs. However, what is the pharmacophore of esculentin in activating Nrf2? A previous study revealed that esculentin exerted an antioxidative function, which might be associated with the phenolic hydroxyl groups (sixth and seventh positions) in the structure.<sup>11</sup> Whether esculentin activates Nrf2 via its chemical structures, such as its phenolic hydroxyl, will be elucidated in our next study.

In this study, we revealed that esculentin activated Nrf2 in IL-1 $\beta$ -treated NPCs. Notably, a previous study also confirmed the activation of Nrf2 by ulinastatin and simethyl fumarate in IL-1 $\beta$ - and LPS-treated NPCs.<sup>29,30</sup> Intriguingly, dimethyl fumarate mitigated LPS-induced oxidative stress and inflammation in NPCs via the Nrf2/HO-1 axis.<sup>23</sup> Additionally, ulinastatin IL-1 $\beta$ -induced apoptosis, oxidative stress, and ECM degradation in NPCs via the Nrf2/HO-1 signaling pathway.<sup>29</sup> Of interest, our data confirmed that blockage of the Nrf2 signaling overturned the protective effects of esculentin on IL-1 $\beta$ -induced apoptosis, ECM degradation and inflammation in NPCs via the Nrf2/HO-1 signaling, indicating that esculentin could attenuate oxidative injury, matrix metabolism dysfunction and inflammation in IL-1 $\beta$ -treated NPCs by the Nrf2/HO-1/NF- $\kappa$ B signaling. Moreover, esculentin was proven to have little toxicity in NPCs. Intriguingly, activating the Nrf2 signaling ameliorates the dysfunction of NPC and the progression of IVDD.<sup>29,30,41</sup> In this study, inhibition of Nrf2 overturned the suppressive effects of esculentin on the IL-1 $\beta$ -induced activation of the NF- $\kappa$ B pathway, indicating that esculentin may restrain the IL-1 $\beta$ -induced activation of the NF- $\kappa$ B signaling by activating the Nrf2/HO-1 axis. The previous study revealed that Nrf2 could adversely affect the NF- $\kappa$ B signaling via several mechanisms to control cellular response during stress and inflammatory situations.<sup>38,42</sup> For instance, Nrf2 hinders oxidative stress-induced NF- $\kappa$ B activation by inhibiting intracellular ROS levels.<sup>42</sup> Moreover, esculentin can enhance Nrf2 expression to prevent I $\kappa$ B $\alpha$  degradation, leading to the inhibition of NF- $\kappa$ B nuclear translocation in macrophages.<sup>38</sup> Therefore, in this study, whether the degradation of I $\kappa$ B $\alpha$  or ROS accumulation is involved in Nrf2-mediated inhibition of the NF- $\kappa$ B pathway. This question will be further

explored in our future work. Collectively, the current data revealed little cytotoxicity of esculetin in HNPCs. Furthermore, esculetin protects against IL-1 $\beta$ -induced oxidative injury, matrix metabolic dysfunction, and inflammatory response by blocking the NF- $\kappa$ B signaling via the activation of the Nrf2/HO-1 axis. Thus, esculetin may ameliorate the progression of IVDD by regulating the dysfunction of NPCs. Together, the current findings may highlight a promising therapeutic agent for IVDD. However, whether esculetin can ameliorate the progression of IVDD *in vivo* remains unclear. In our next study, we will construct the IVDD animal model to explore the potential roles of esculetin in the animal model. The effects of esculetin on inflammatory response, NPC injury, and matrix metabolic disruption will be analyzed *in vivo*. Furthermore, the involvement of the Nrf2/HO-1 axis will also be investigated in animal experiments.

## ■ ASSOCIATED CONTENT

### Data Availability Statement

All data generated or analyzed during this study are included in this published article.

## ■ AUTHOR INFORMATION

### Corresponding Author

Yiqi Wu – Department of Spinal Surgery, Longyan First Affiliated Hospital of Fujian Medical University, Longyan 364000, P. R. China; [orcid.org/0000-0003-0994-7842](https://orcid.org/0000-0003-0994-7842); Phone: 86-13950806111; Email: [Wuyiqi0597@hotmail.com](mailto:Wuyiqi0597@hotmail.com)

### Authors

Chunhui Huang – Department of Spinal Surgery, Longyan First Affiliated Hospital of Fujian Medical University, Longyan 364000, P. R. China

Kaiwei Zou – Department of Spinal Surgery, Longyan First Affiliated Hospital of Fujian Medical University, Longyan 364000, P. R. China

Yizhang Wang – Department of Cardiology, Longyan First Affiliated Hospital of Fujian Medical University, Longyan 364000, P. R. China

Kai Tang – Department of Spinal Surgery, Longyan First Affiliated Hospital of Fujian Medical University, Longyan 364000, P. R. China

Complete contact information is available at: <https://pubs.acs.org/10.1021/acsomega.3c06771>

### Author Contributions

<sup>§</sup>C.H. and K.Z. contributed equally, and all authors agreed to define them as co-first authors. C.H. was responsible for the methodology, software, validation, data curation, and writing of the original draft. K.Z. performed the methodology, software, formal analysis, data curation, and validation. Y. Wang was responsible for the data curation, software, validation, methodology, and formal analysis. K.T. performed the methodology, software, formal analysis, data curation, and validation. Y. Wu was responsible for the conceptualization, data curation, formal analysis, methodology, investigation, and supervision. All authors have read and approved the final manuscript.

### Notes

The authors declare no competing financial interest.

## ■ REFERENCES

- (1) Manchikanti, L.; Singh, V.; Falco, F. J.; Benyamin, R. M.; Hirsch, J. A. Epidemiology of low back pain in adults. *Neuromodulation* **2014**, *17* (Suppl 2), 3–10.
- (2) de Souza, I. M. B.; Sakaguchi, T. F.; Yuan, S. L. K.; Matsutani, L. A.; do Espirito-Santo, A. S.; Pereira, C. A. B.; Marques, A. P. Prevalence of low back pain in the elderly population: a systematic review. *Clinics* **2019**, *74*, No. e789.
- (3) Dagenais, S.; Caro, J.; Haldeman, S. A systematic review of low back pain cost of illness studies in the United States and internationally. *Spine J.* **2008**, *8*, 8–20.
- (4) Itoh, H.; Kitamura, F.; Yokoyama, K. Estimates of annual medical costs of work-related low back pain in Japan. *Ind. Health* **2013**, *51*, 524–529.
- (5) Khan, A. N.; Jacobsen, H. E.; Khan, J.; Filippi, C. G.; Levine, M.; Lehman, R. A., Jr.; Riew, K. D.; Lenke, L. G.; Chahine, N. O. Inflammatory biomarkers of low back pain and disc degeneration: a review. *Ann. N. Y. Acad. Sci.* **2017**, *1410*, 68–84.
- (6) Chen, J.; Xuan, J.; Gu, Y. T.; Shi, K. S.; Xie, J. J.; Chen, J. X.; Zheng, Z. M.; Chen, Y.; Chen, X. B.; Wu, Y. S.; Zhang, X. L.; Wang, X. Y. Celastrol reduces IL-1 $\beta$  induced matrix catabolism, oxidative stress and inflammation in human nucleus pulposus cells and attenuates rat intervertebral disc degeneration *in vivo*. *Biomed. Pharmacother.* **2017**, *91*, 208–219.
- (7) Zhang, G.-Z.; Liu, M. Q.; Chen, H. W.; Wu, Z. L.; Gao, Y. C.; Ma, Z. J.; He, X. G.; Kang, X. W. NF- $\kappa$ B signalling pathways in nucleus pulposus cell function and intervertebral disc degeneration. *Cell Prolif.* **2021**, *54*, No. e13057, DOI: [10.1111/cpr.13057](https://doi.org/10.1111/cpr.13057).
- (8) Le Maitre, C. L.; Freemont, A. J.; Hoyland, J. A. The role of interleukin-1 in the pathogenesis of human intervertebral disc degeneration. *Arthritis Res. Ther.* **2005**, *7*, R732–745.
- (9) Risbud, M. V.; Shapiro, I. M. Role of cytokines in intervertebral disc degeneration: pain and disc content. *Nat. Rev. Rheumatol.* **2014**, *10*, 44–56.
- (10) Zhang, Y.; He, F.; Chen, Z.; Su, Q.; Yan, M.; Zhang, Q.; Tan, J.; Qian, L.; Han, Y. Melatonin modulates IL-1 $\beta$ -induced extracellular matrix remodeling in human nucleus pulposus cells and attenuates rat intervertebral disc degeneration and inflammation. *Aging* **2019**, *11*, 10499–10512.
- (11) Zhang, L.; Xie, Q.; Li, X. Esculetin: A review of its pharmacology and pharmacokinetics. *Phytother. Res.* **2022**, *36*, 279–298.
- (12) He, Y.; Li, C.; Ma, Q.; Chen, S. Esculetin inhibits oxidative stress and apoptosis in H9c2 cardiomyocytes following hypoxia/reoxygenation injury. *Biochem. Biophys. Res. Commun.* **2018**, *501*, 139–144.
- (13) Xu, F.; Li, X.; Liu, L.; Xiao, X.; Zhang, L.; Zhang, S.; Lin, P.; Wang, X.; Wang, Y.; Li, Q. Attenuation of doxorubicin-induced cardiotoxicity by esculetin through modulation of Bmi-1 expression. *Exp. Ther. Med.* **2017**, *14*, 2216–2220.
- (14) Lee, C. R.; Shin, E. J.; Kim, H. C.; Choi, Y. S.; Shin, T.; Wie, M. B. Esculetin inhibits N-methyl-D-aspartate neurotoxicity via glutathione preservation in primary cortical cultures. *Lab. Anim. Res.* **2011**, *27*, 259–263.
- (15) Lee, H. C.; Liu, F. C.; Tsai, C. N.; Chou, A. H.; Liao, C. C.; Yu, H. P. Esculetin Ameliorates Lipopolysaccharide-Induced Acute Lung Injury in Mice Via Modulation of the AKT/ERK/NF- $\kappa$ B and ROR $\gamma$ mat/IL-17 Pathways. *Inflammation* **2020**, *43*, 962–974.
- (16) Witacenis, A.; Seito, L. N.; Di Stasi, L. C. Intestinal anti-inflammatory activity of esculetin and 4-methyl-esculetin in the trinitrobenzenesulphonic acid model of rat colitis. *Chem.–Biol. Interact.* **2010**, *186*, 211–218.
- (17) Cheng, Y. J.; Tian, X. L.; Zeng, Y. Z.; Lan, N.; Guo, L. F.; Liu, K. F.; Fang, H. L.; Fan, H. Y.; Peng, Z. L. Esculetin protects against early sepsis via attenuating inflammation by inhibiting NF- $\kappa$ B and STAT1/STAT3 signaling. *Chin. J. Nat. Med.* **2021**, *19*, 432–441, DOI: [10.1016/S1875-5364\(21\)60042-0](https://doi.org/10.1016/S1875-5364(21)60042-0).
- (18) Rzdokiewicz, P.; Gasinska, E.; Maslinski, S.; Bujalska-Zadrozny, M. Antinociceptive properties of esculetin in non-inflammatory and

inflammatory models of pain in rats. *Clin. Exp. Pharmacol. Physiol.* **2015**, *42*, 213–219.

(19) Jayakumar, T.; Huang, C. J.; Yen, T. L.; Hsia, C. W.; Sheu, J. R.; Bhavan, P. S.; Huang, W. C.; Hsieh, C. Y.; Hsia, C. H. Activation of Nrf2 by Esculetin Mitigates Inflammatory Responses through Suppression of NF-kappaB Signaling Cascade in RAW 264.7 Cells. *Molecules* **2022**, *27*, 5143.

(20) Yamada, H.; Watanabe, K.; Saito, T.; Hayashi, H.; Niitani, Y.; Kikuchi, T.; Ito, A.; Fujikawa, K.; Lohmander, L. S. Esculetin (dihydroxycoumarin) inhibits the production of matrix metalloproteinases in cartilage explants, and oral administration of its prodrug, CPA-926, suppresses cartilage destruction in rabbit experimental osteoarthritis. *J. Rheumatol.* **1999**, *26*, 654–662.

(21) Yu, L.; Wang, Z.; Mo, Z.; Zou, B.; Yang, Y.; Sun, R.; Ma, W.; Yu, M.; Zhang, S.; Yu, Z. Synergetic delivery of triptolide and Ce6 with light-activatable liposomes for efficient hepatocellular carcinoma therapy. *Acta Pharm. Sin. B* **2021**, *11*, 2004–2015.

(22) He, M.; Yu, L.; Yang, Y.; Zou, B.; Ma, W.; Yu, M.; Lu, J.; Xiong, G.; Yu, Z.; Li, A. Delivery of triptolide with reduction-sensitive polymer nanoparticles for liver cancer therapy on patient-derived xenografts models. *Chin. Chem. Lett.* **2020**, *31*, 3178–3182.

(23) Yang, Y.; Liu, X.; Ma, W.; Xu, Q.; Chen, G.; Wang, Y.; Xiao, H.; Li, N.; Liang, X. J.; Yu, M.; Yu, Z. Light-activatable liposomes for repetitive on-demand drug release and immunopotentiality in hypoxic tumor therapy. *Biomaterials* **2021**, *265*, No. 120456.

(24) Chen, G.; Yang, Y.; Xu, Q.; Ling, M.; Lin, H.; Ma, W.; Sun, R.; Xu, Y.; Liu, X.; Li, N.; Yu, Z.; Yu, M. Self-Amplification of Tumor Oxidative Stress with Degradable Metallic Complexes for Synergistic Cascade Tumor Therapy. *Nano Lett.* **2020**, *20*, 8141–8150.

(25) Ma, W.; Chen, Q.; Xu, W.; Yu, M.; Yang, Y.; Zou, B.; Zhang, Y. S.; Ding, J.; Yu, Z. Self-targeting visualizable hyaluronate nanogel for synchronized intracellular release of doxorubicin and cisplatin in combating multidrug-resistant breast cancer. *Nano Res.* **2021**, *14*, 846–857.

(26) Yang, Y.; Yu, Y.; Chen, H.; Meng, X.; Ma, W.; Yu, M.; Li, Z.; Li, C.; Liu, H.; Zhang, X.; Xiao, H.; Yu, Z. Illuminating Platinum Transportation while Maximizing Therapeutic Efficacy by Gold Nanoclusters via Simultaneous Near-Infrared-I/II Imaging and Glutathione Scavenging. *ACS Nano* **2020**, *14*, 13536–13547.

(27) Li, L.; Wei, K.; Ding, Y.; Ahati, P.; Xu, H.; Fang, H.; Wang, H. M2a Macrophage-Secreted CHI3L1 Promotes Extracellular Matrix Metabolic Imbalances via Activation of IL-13Ralpha2/MAPK Pathway in Rat Intervertebral Disc Degeneration. *Front. Immunol.* **2021**, *12*, No. 666361.

(28) Tsingas, M.; Ottone, O. K.; Haseeb, A.; Barve, R. A.; Shapiro, I. M.; Lefebvre, V.; Risbud, M. V. Sox9 deletion causes severe intervertebral disc degeneration characterized by apoptosis, matrix remodeling, and compartment-specific transcriptomic changes. *Matrix Biol.* **2020**, *94*, 110–133.

(29) Luo, X.; Huan, L.; Lin, F.; Kong, F.; Sun, X.; Li, F.; Zhu, J.; Sun, J.; Xu, X.; Sun, K.; Duan, L.; Shi, J. Ulinastatin Ameliorates IL-1beta-Induced Cell Dysfunction in Human Nucleus Pulposus Cells via Nrf2/NF-kappaB Pathway. *Oxid. Med. Longevity* **2021**, *2021*, No. 5558687, DOI: 10.1155/2021/5558687.

(30) Wang, R.; Luo, D.; Li, Z.; Han, H. Dimethyl Fumarate Ameliorates Nucleus Pulposus Cell Dysfunction through Activating the Nrf2/HO-1 Pathway in Intervertebral Disc Degeneration. *Comput. Math. Methods Med.* **2021**, *2021*, No. 6021763.

(31) Zhang, G. Z.; Deng, Y. J.; Xie, Q. Q.; Ren, E. H.; Ma, Z. J.; He, X. G.; Gao, Y. C.; Kang, X. W. Sirtuins and intervertebral disc degeneration: Roles in inflammation, oxidative stress, and mitochondrial function. *Clin. Chim. Acta* **2020**, *508*, 33–42.

(32) Yang, M.; Peng, Y.; Liu, W.; Zhou, M.; Meng, Q.; Yuan, C. Sirtuin 2 expression suppresses oxidative stress and senescence of nucleus pulposus cells through inhibition of the p53/p21 pathway. *Biochem. Biophys. Res. Commun.* **2019**, *513*, 616–622.

(33) Zhou, T. Y.; Wu, Y. G.; Zhang, Y. Z.; Bao, Y. W.; Zhao, Y. SIRT3 retards intervertebral disc degeneration by anti-oxidative stress

by activating the SIRT3/FOXO3/SOD2 signaling pathway. *Eur. Rev. Med. Pharmacol. Sci.* **2019**, *23*, 9180–9188.

(34) Watanabe, K.; Ito, A.; Sato, T.; Saito, T.; Hayashi, H.; Niitani, Y. Esculetin suppresses proteoglycan metabolism by inhibiting the production of matrix metalloproteinases in rabbit chondrocytes. *Eur. J. Pharmacol.* **1999**, *370*, 297–305.

(35) Chen, M.; Sun, Y.; Liu, H. Cell membrane biomimetic nanomedicines for cancer phototherapy. *Interdiscip. Med.* **2023**, *1*, No. e20220012.

(36) Xia, C.; Zeng, Z.; Fang, B.; Tao, M.; Gu, C.; Zheng, L.; Wang, Y.; Shi, Y.; Fang, C.; Mei, S.; Chen, Q.; Zhao, J.; Lin, X.; Fan, S.; Jin, Y.; Chen, P. Mesenchymal stem cell-derived exosomes ameliorate intervertebral disc degeneration via anti-oxidant and anti-inflammatory effects. *Free Radical Biol. Med.* **2019**, *143*, 1–15.

(37) Navone, S. E.; Marfia, G.; Giannoni, A.; Beretta, M.; Guarnaccia, L.; Gualtierotti, R.; Nicoli, D.; Rampini, P.; Campanella, R. Inflammatory mediators and signalling pathways controlling intervertebral disc degeneration. *Histol. Histopathol.* **2017**, *32*, 523–542.

(38) Lin, Y.; Tang, G.; Jiao, Y.; Yuan, Y.; Zheng, Y.; Chen, Y.; Xiao, J.; Li, C.; Chen, Z.; Cao, P. Propionibacterium acnes Induces Intervertebral Disc Degeneration by Promoting iNOS/NO and COX-2/PGE(2) Activation via the ROS-Dependent NF-kappaB Pathway. *Oxid. Med. Cell. Longevity* **2018**, *2018*, No. 3692752, DOI: 10.1155/2018/3692752.

(39) Ozal, S. A.; Turkecul, K.; Gurlu, V.; Guclu, H.; Erdogan, S. Esculetin Protects Human Retinal Pigment Epithelial Cells from Lipopolysaccharide-induced Inflammation and Cell Death. *Curr. Eye Res.* **2018**, *43*, 1169–1176.

(40) Zhao, Z.; Wang, X.; Zhang, R.; Ma, B.; Niu, S.; Di, X.; Ni, L.; Liu, C. Melatonin attenuates smoking-induced atherosclerosis by activating the Nrf2 pathway via NLRP3 inflammasomes in endothelial cells. *Aging* **2021**, *13*, 11363–11380.

(41) Shao, Z.; Wang, B.; Shi, Y.; Xie, C.; Huang, C.; Chen, B.; Zhang, H.; Zeng, G.; Liang, H.; Wu, Y.; Zhou, Y.; Tian, N.; Wu, A.; Gao, W.; Wang, X.; Zhang, X. Senolytic agent Quercetin ameliorates intervertebral disc degeneration via the Nrf2/NF-kappaB axis. *Osteoarthritis Cartilage* **2021**, *29*, 413–422.

(42) Soares, M. P.; Seldon, M. P.; Gregoire, I. P.; Vassilevskaia, T.; Berberat, P. O.; Yu, J.; Tsui, T. Y.; Bach, F. H. Heme oxygenase-1 modulates the expression of adhesion molecules associated with endothelial cell activation. *J. Immunol.* **2004**, *172*, 3553–3563.